AIAA 2000-0645
PARTICLE VAPORIZATION VELOCIMETRY FOR SOOT-CONTAINING FLOWS

P. Yang and J. M. Seitzman
Georgia Institute of Technology
Atlanta, GA

R. T. Wainner
US Army Research Laboratory
Aberdeen Proving Grounds, MD

38th Aerospace Sciences Meeting & Exhibit
10-13 January 2000 / Reno, NV

AIAA-2000-0645

PARTICLE VAPORIZATION VELOCIMETRY FOR SOOT-CONTAINING FLOWS

P. Yang* and J. M. Seitzman†

Georgia Institute of Technology
Aerospace Combustion Laboratory
School of Aerospace Engineering
Atlanta, GA 30332-0150

R. T. Wainner‡

US Army Research Laboratory
AMSRL-WM-BD
Aberdeen Proving Grounds, MD 21005-5066

Abstract

We characterize a novel imaging technique for velocity measurements in particle laden flows. The technique, Particle Vaporization Velocimetry (PVV), is a form of flow tagging based on laser vaporization of absorbing particles at defined locations in the flow. The locations of these tagged regions are then interrogated after a known delay to determine the convective velocity. Results are presented for vaporization of carbonaceous particles in a heated, nonreacting gas jet and a hydrocarbon-air diffusion flame. While the flame produces its own carbon particles (soot), the nonreacting gas get is seeded with submicron-sized, carbon black particles. Interrogation is provided by either elastic scattering or laser-induced incandescence from the soot. The results are similar for the two very different flows, indicating that the PVV technique should be applicable to a wide range of environments. The laser fluence required to produce the tagged region for soot is on the order of the threshold fluence required for laser-induced incandescence measurements, though with a somewhat lower value for scattering detection. The tag lifetime for the current systems exceeds 10 ms, and should be limited only by turbulent mixing in practical flows.

Introduction

Measurement of particle velocities can be of great utility in a wide range of flows. For example in hydrocarbon-based combustion flows, small carbonaceous particles, commonly referred to as soot, are formed. Soot particles result from non-oxidizing reactions of the fuel molecules and are destroyed if sufficient oxidation occurs in the flame. Soot particles are important due to their impact on human health, the environment, and the performance of energy conversion devices.[1-4] Thus, there is an interest both in monitoring soot from combustion devices, such as diesel and aircraft turbine engines, and for measurements that lead to a better understanding of the processes by which soot is created and destroyed.

Established techniques exist for measuring soot properties, such as soot concentration and soot particle size(s). These have included physical sampling,[5,6] and laser scattering and extinction.[7,8] None of these alone, however, possess the combined attributes of nonintrusiveness, fine spatial resolution and weak dependence on particle size for concentration measurements. More recently, laser-induced incandescence (LII) has been studied as a diagnostic tool for soot measurements in flames,[9-12] engines[13,14] and exhaust flows.[15-1617] LII combines the best characteristics of some of the more established optical techniques. Like elastic scattering, LII is an imaging technique with excellent spatial resolution, and it provides a strong signal. Since the signal primarily corresponds to the amount of laser energy absorbed, LII, like extinction, is mostly sensitive to the soot mass concentration (or volume fraction for a known soot density). Extensions of LII have also been developed for particle size measurements.[18,19]

Combining these powerful existing techniques for soot concentration and particle size with measurements of soot particle velocities could then be used to determine quantities like local soot mass flux and soot

*Graduate Research Assistant

†Assistant Professor, Senior Member AIAA

‡Member AIAA (work performed while at GIT)

production/oxidation rates. A number of nonintrusive, optical techniques have been developed for velocity measurement where there is a single particle in the detection volume, or in a pixel for imaging methods. These include Laser Doppler Velocimetry[20] (LDV) and Particle Image Velocimetry[21,22] (PIV), with the latter providing two-dimensional maps (planes) of velocity. Unfortunately, these methods have limited applicability in flows with dense particle loadings. For particles no bigger than 100 nm and generously small measurement volumes, both LDV and PIV are generally limited to particle volume fractions below 0.1-1 ppb. In addition, these techniques can not generally be used to discriminate between particles of different elemental composition; all particles that elastically scatter contribute to the signal.

For gas velocity measurements, a number of other optical techniques have been developed to remove the need for particle seeding. A number of these can be categorized as flow tagging velocimetry,[23-25] in which regions of the flow (a line, crossing lines, grids, etc.) are marked at some initial time, and the location of the marked regions are interrogated at some known delay, usually by a planar imaging technique. The displacement of the regions is used to determine the velocity component(s) in the plane of the imaging sheet.

Particle Vaporization Velocimetry (PVV) extends these flow tagging approaches to particle velocity measurements. In this paper, we describe PVV and report experimental results that characterize the method for soot particle velocity measurements. Results are obtained from two environments, a high-temperature reacting flow and the other a low temperature (~400 K) nonreacting flow. The experiments are intended to investigate the laser fluence required to perform PVV and the lifetime of the tagged region in these two very different environments.

Description of PVV

In particle vaporization velocimetry, the marked region is produced by laser vaporization of sufficiently absorbing particles. In general, such particles are rapidly heated when exposed to a pulsed laser. In the case of soot if the laser intensity is sufficiently high, the particles are heated to a point where vaporization becomes important (~4000 K). This is the same approach used for LII measurements, since at this threshold fluence, the broadband incandescence from the high temperature particle is easily detected over the unheated particle incandescence and flame luminosity. For illustration, Figure 1 shows a typical dependence of the LII signal on laser fluence, with the peak incandescence occurring near the point where vaporization becomes the dominant energy loss mechanism.

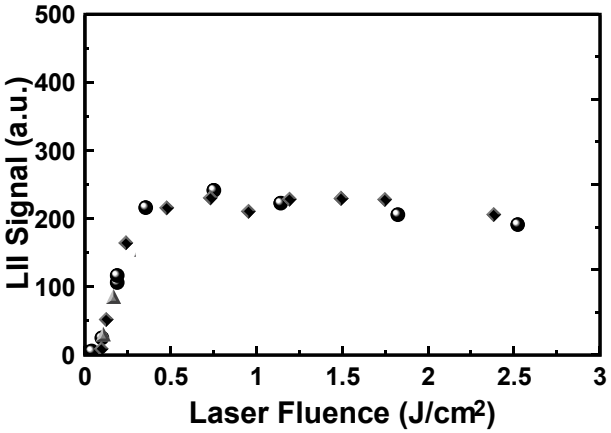

Figure 1. Variation of LII signal with laser fluence for measurements acquired in a laminar, ethylene-air laminar diffusion flame, 25 mm above the fuel-tube exit, with laser excitation from a pulsed Nd:YAG laser (1064 nm) and a 50 ns detection gate beginning at the onset of the laser pulse.

For laser fluences sufficiently above this threshold value (~0.5-0.6 J/cm^2 for the 1064 nm laser results shown in Figure 1), the particles can be almost completely vaporized,[26] producing a region of reduced particle concentration. Once this tagged region (hole) is produced, at least two methods amenable to planar imaging can be used to track its location: elastic scattering and LII. In both, the marked area is seen as a reduced signal. Since PVV tracks regions of vaporized particles, it can be employed at high particle loadings. PVV tracks the particle velocities, which for small particles can correspond to the gas velocity under a wide range of conditions. Also, a system designed for LII imaging can easily be adapted for velocity measurements, even simultaneous mass concentration (from the LII signal of the marking pulse) and velocity measurements that would permit determination of local soot mass flux (or a component of the flux).

Experimental Methods

Flowfields

The PVV velocity measurements are acquired in two axisymmetric (round) jet flows. One is a laminar diffusion flame, and the other is an exhaust-like, nonreacting, heated jet. The axisymmetric diffusion flame has been used extensively in a number of soot studies.[27] In this burner, fuel flows through a central tube of 11.1

mm i.d., surrounded by a concentric flow of air contained in a 101.6 mm i.d. honeycombed outer tube. Ethylene (C_2H_4) was chosen as the fuel for its high sooting tendency. The flowrates for fuel and air, respectively, were 3.85 cm^3/s and 713.3 cm^3/s, measured by calibrated rotameters. The resulting ~80 mm tall flame has a peak soot volume fractions of nearly 10 ppm. Measurements were obtained in the flame with the marking laser located 10, 20, 30 and 40 mm above the fuel tube exit. For these measurements, the flame location was controlled with a three-axis translation stage, while the laser and imaging locations remain fixed.

The nonreacting flow is produced by a soot aerosol generator.[16] The exhaust contains small, roughly spherical agglomerates (<400 nm diameter) composed of ~17 nm carbon black primary particles (Cabot 800). These carbon black agglomerates do not have the same morphology as the branchy soot particles typically found in flames. They should, however, correspond in many ways to aged soot particles in a flame exhaust, since the carbon black particles are produced in a similar process. The exhaust from the soot generator primarily consists of heated air (~400 K) with 4.4% water vapor by volume, and flows at 9.5 slpm (measured by calibrated rotameters). Measurements were acquired for two soot volume fractions, 0.4 and 4.0 ppb, having different "soot" average diameters (D_{10} of 136 and 294 nm) for the two cases. The carbon aerosol exits a 17 mm diam., 300 mm long cylinder, with the marking laser located 10 mm above the exit of this tube.

Optical Systems

A schematic of the optical arrangement is shown in Figure 2. The marking (first) and readout (second) laser pulses are produced by a dual-oscillator, Q-switched, 10 Hz Nd:YAG system (Continuum Surelite-I PIV). Both beam are converted into laser sheets, which are aligned normal to one another in the flow. They also propagate at a small relative angle, crossing near the center of the imaged region.

The fundamental infrared output of one of the laser oscillators, with a maximum pulse energy of 450 mJ, is used as the marking beam. The 8 mm (full width) diameter beam is focused by a 280 mm focal length cylindrical lens to a horizontal laser sheet. The focus of the 8 mm wide sheet is typically located past the flow, such that the sheet thickness decreases slightly from the point where it first encounters the flow. The nominal thickness (FWHM) in the flame measurements is 0.45 mm, and changes to 0.6 mm for the nonreacting flow. In addition, the sheet width can be reduced from 8 mm to 2 mm using a metallic aperture placed behind the focusing lens (see Figure 2). The thin dimension (thickness) of the sheet is parallel to the primary flow direction. The marking laser energy is varied with a half-wave plate and polarizing beam splitter.

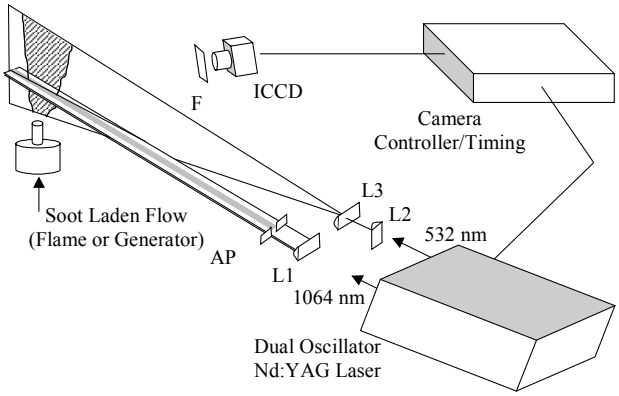

Figure 2. Optical setup for PVV measurements in both the flame and soot generator; L1: 280 mm cylindrical lens; L2: 500 mm cyl.; L3: 200 mm cyl.; AP: metallic aperture; F: filter(s).

The readout beam is produced by the frequency-doubled (532 nm) output of the second laser head, with a maximum pulse energy of 200 mJ. The image beam is focused by a 500 mm focal length, cylindrical lens in the vertical direction and spread in the horizontal direction by a 25 mm cylindrical lens. This yields an imaging sheet that is ~0.4 mm thick and 100 mm high. The fluence of the imaging beam is fixed for all measurements at ~0.4 J/cm^2, which is sufficient to allow either LII or scattering measurements of the nonvaporized particles. The pulse-to-pulse repeatability of the energy is less than $\pm$ 5% for both lasers.

The LII and elastic scattering images are recorded at roughly 45° to the propagation direction of the visible laser sheet (rather than the preferred 90° due to limited optical access) by an intensified CCD camera (Princeton Instruments ICCD, 576×384) equipped with a standard 35mm camera lens. For the soot generator, with its low particle concentrations, the lens f-number is set to its minimum value for the LII measurements (f/2.8), but degraded for the brighter scattering measurements. In the flame, with its higher levels of soot, the lens aperture is increased to f/32 for both interrogation methods, and neutral density filters are placed in front of the lens for the scattering case to prevent intensifier saturation. The intensifier gate duration is 50 ns, and for the scattering data, it begins just after the onset of the interrogation laser pulse For the LII measure-

ments, the bright elastic scattering signal can rejected either by placing a 532 nm holographic notch filter in front of the lens, or delaying the intensifier gate by 32 ns. Since the total duration of the laser pulse is about 25 ns, the delayed gating rejects the prompt scattering signal, but is sufficient to detect the longer lived LII.

Results

PVV Measurements with LII Detection

Figure 3 shows LII images acquired in the diffusion flame with the marking beam 40 mm above the burner exit. This location corresponds to the peak soot concentration, nearly 10 ppm occurring near the edge of the flame. Above this point, soot production is low at the outer regions of the flame, outpaced by oxidation. Based on the movement of the tagged region between the 10 μs and 1 ms images, the measured velocity at 40 mm height in the peak soot region is 1.8 m/s. This compares well to a value of 1.7 m/s from interpolated LDV measurements.[27] For the 1 ms delay and for the image magnification used here (12.7 pixels per millimeter), the estimated PVV velocity resolution is 0.04-0.08 m/s, assuming the uncertainty in locating the center of the marked region is one-half to one pixel.

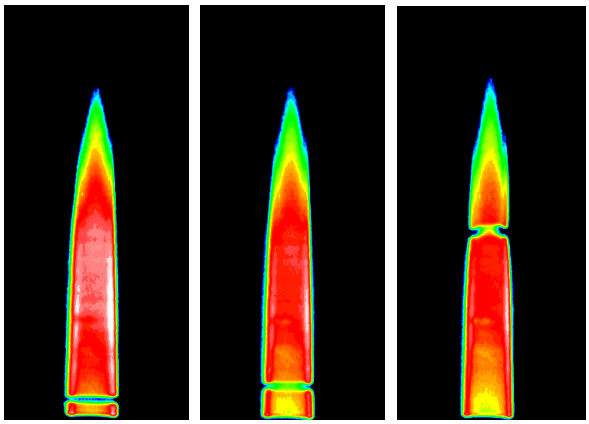

(a) **(b)** **(c)**

Figure 3. Average (100 shot) LII images (21×46 mm) of the vaporized stripe acquired in the diffusion flame for three delays: a) 10 μs, b) 1 ms, and c) 10 ms after the 8 mm wide marking laser sheet pulse; which passes 40 mm above the fuel tube exit (this is the location shown in (a)).

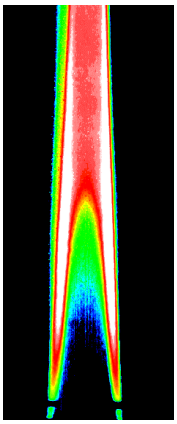

Figure 4. Average (100 shot) LII image (21×46 mm) of the vaporized stripe acquired in the diffusion flame with the marking laser 10 mm above the marking laser sheet and for a 10 μs delay.

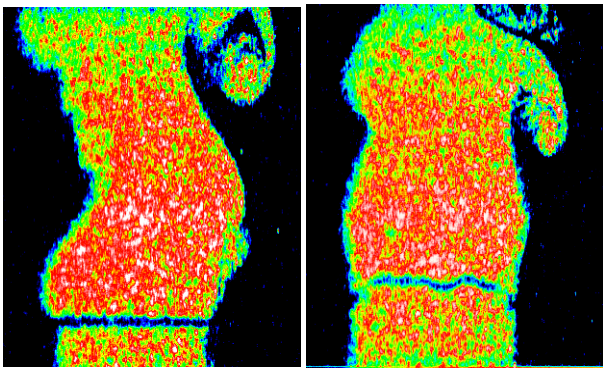

(a) **(b)**

Figure 5. Instantaneous LII images (26×32 mm) of the vaporized stripe acquired in the 4 ppb soot exhaust for two delays after the marking laser pulse: a) 10 μs and b) 1 ms.

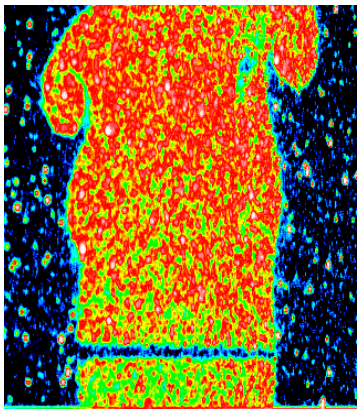

Figure 6. Instantaneous elastic scattering image (26×32 mm) of the vaporized stripe acquired in the 4 ppb soot exhaust for a 10 μs delay after the marking laser pulse and with f/11 detection.

Figure 4 shows a similar result for an LII image acquired with the marking sheet at the lowest height (10 mm above the fuel exit). In this lower part of the flame, soot axial velocities can only be measured in a region near the edge of the central fuel jet, since little soot exists within the flame. The peak soot concentration is near 1 ppm here, and soot production rates are expected to be much higher than at 40 mm. The measured velocity is 0.8 m/s, as compared to a values of 0.7 m/s from the LDV results.

Figure 5 shows example of LII images in the 4 ppb soot generator exhaust with the tagged region visible in the lower portion of the images. The results for the 0.4 ppb case are similar, albeit with signals roughly 10 times lower. The velocity measured from this LII image, 2.7 m/s, compares well with the value of 2.8 m/s calculated from the volumetric flowrate measured by the rotameters.

Scattering Detection

The results for scattering detection are similar to the LII PVV data. Figure 6 shows a scattering counterpart to the LII image of Figure 5a. The first thing to note is the increased signal outside the jet, due to elastic scattering by dust particles in the room air. This is the biggest potential drawback to scattering detection, rejection of other scattering particles or bodies. For the flame however, with its much higher soot levels ($\times 10^3$), the dust scattering is negligible.

The main advantage of scattering detection for PVV is its higher photon yield. In both the soot generator and the flame, the scattering signal is much stronger than the LII signal. It should be noted, though, that the ICCD is not optimized for detection of LII. A large portion of the LII signal occurs at wavelengths longer than 600 nm, where the photocathode quantum efficiency of the ICCD decays rapidly.

Correcting for the added ND filter in the case of the scattering images (ND=2.6), the scattering to LII ratio in the flame is 100-200. In the soot generator, the ratio decreases to 30-60. The primary difference in the two systems is the effective particle size, with the soot generator producing larger, more spherical agglomerates. Although the larger particles found in the soot generator should produce more scattering (per ppm of soot), the increase in LII signal with particle size[16] is likely greater. Other differences between the two carbon particles, for example the level of graphitization, may also play some role in the scattering to LII ratio.

In terms of velocity measurement, the scattering images give essentially identical values to the LII images. For example, the velocity in the soot generator from the scattering results (again based on a 1 ms delay) is 2.75 m/s, which is close to the 2.7 ms result from the LII images.

Marking Laser Energy

In flow tagging techniques like PVV, the ability to determine the location of the marked region can often limit the accuracy of the measurement. A quantitative measure of the detectability of the flow tagging is the contrast between the signals from the marked (S_{mark}) and unmarked (S_{unmark}) regions. The contrast can be defined

$$Contrast = \frac{S_{unmark} - S_{mark}}{S_{unmark}} \qquad (1)$$

with the optimal contrast being unity.

The images shown above were obtained with a laser fluences of ~6-8 J/cm^2. Lower fluences are also sufficient to produce a soot "hole." For example, Figure 7 shows the variation in contrast with marking laser fluence in the flame, for both LII and scattering detection. The measured contrast continues to increase with fluence for both methods up to the maximum values employed here (~20 J/cm^2), though there is little change beyond ~2-3 J/cm^2. It is useful to note that this near optimum fluence is only 3-4 times the value normally employed in LII measurements. This would therefore permit soot concentration measurements based on the LII signal from the marking pulse.

The data suggest that at 2-3 J/cm^2 the energy in the center of the roughly Gaussian beam profile is sufficient to nearly completely vaporize the soot particles. The similarity in contrast at the higher laser fluences for both interrogation approaches indicates that the particles are truly vaporized. While LII primarily measures the mass of solid soot, scattering depends on the soot shape and size (see discussion below). The similar contrast response indicates that at the high fluence levels, the first laser pulse is truly vaporizing particles, and not simply shattering them or changing their morphology.

On the other hand, there is a significant difference between scattering and LII detection at lower fluences (<2 J/cm^2), where scattering detection has a higher contrast, and therefore is more detectable. Part of the increased observability for scattering detection could be its improved signal-to-noise ratio, due to its higher photon yield in these shot-noise limited images. This is only a minor effect, since the scattering images were acquired with lower detection efficiencies, so as to keep

the average scattering and LII counts/pixel within a factor of two.

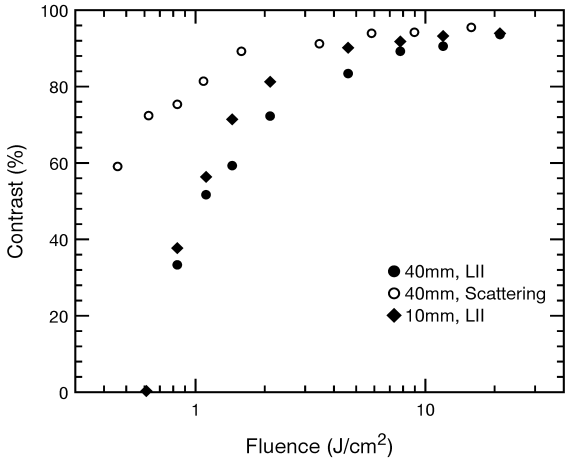

Figure 7. Fluence dependence of the contrast (see Eq. 1) produced by the marking laser in the flame at a 1 μs delay, for two heights and both LII and scattering detection.

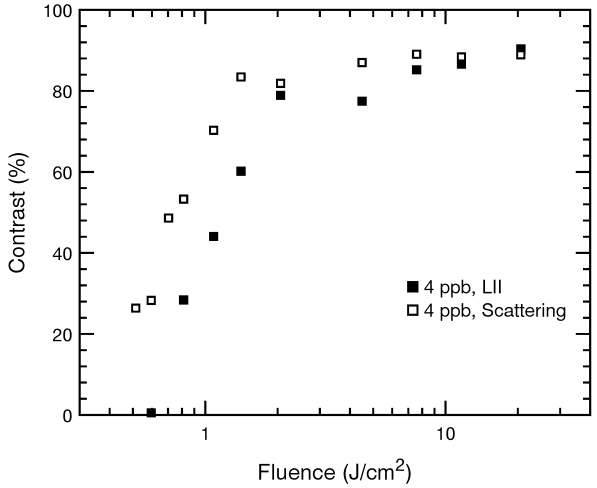

Figure 8. Fluence dependence of the contrast produced by the marking laser in the soot generator with a 1 μs delay for the recording laser, comparing LII and scattering detection.

Another possible source for the difference is the higher sensitivity of the elastic scattering to particle size. In the case of Rayleigh scattering, the signal per particle scales like the particle diameter to the sixth-power, i.e., D^6. The LII signal scales more like the particle volume, i.e., D^3. Therefore, small amounts of mass loss by a particle should decrease the scattering signal much more significantly than the LII signal.

However, the extreme difference between the measured contrasts at fluences below 0.6-0.7 J/cm^2 suggests another option. Recall that previous LII results (for example see Figure 1) suggest fluence values below 0.5-0.6 J/cm^2 are not likely to produce significant soot vaporization. This is consistent with the lack of contrast in the LII detection at 0.6 J/cm^2. At this and lower fluences, however, the scattering detection shows a relatively large contrast (0.6-0.7). If the LII signal indicates little vaporization by the marking laser, then the scattering result suggests some kind of particle fragmentation may be occurring.

Similar fluence behavior was observed in the soot generator, as illustrated in Figure 8. Again both detection methods show a similar contrast for fluences above ~2 J/cm^2. For fluences of 0.6-1 J/cm^2, the scattering detection has a markedly higher contrast, due to the higher particle size sensitivity of the scattering and the possible shattering of the soot agglomerates, probably after the first laser pulse ends.

Tagged Region Lifetime

Tagging-based velocimetry techniques are often limited to high speed flow measurements, due to the short lifetimes of the molecular tags employed. The shorter the tag lifetime, the faster the velocity has to be for the tagged region to move a measurable distance. For our particle tagging approach, the ultimate tag lifetime can be longer than for molecular tags, because particles experience less diffusion than gas molecules. The measured tag lifetimes were measured in both flows, by varying the time delay between the marking and readout lasers. The measured lifetimes, again quantified by the contrast, are shown in Figure 9 (flame) and Figure 10 (soot generator exhaust).

In both environments, the lifetime of the tagged "hole" is at least 3 ms. In the higher region (40 mm) of the steady flame, the contrast remains essentially unchanged (> 90%) up to 10 ms, the largest delay studied. In the soot generator, with its more unsteady flow (see Figure 5), the contrast degrades somewhat at the longer delays, though it remains above 60% even at 3 ms. In both these regions, the tag lifetime appears to be limited by flow unsteadiness and small-scale velocity fluctuations, which are significantly reduced in the much steadier, laminar flame. In these regions, there is no indication that the vaporized soot material reforms into solid particles in any significant amount (at least in the millisecond time scales here). This conclusion is supported by the agreement between the LII and scattering results in both the flame and soot generator. Even if small particles were reforming, they should be detected

in the LII measurement, which is not strongly sensitive to particle size.

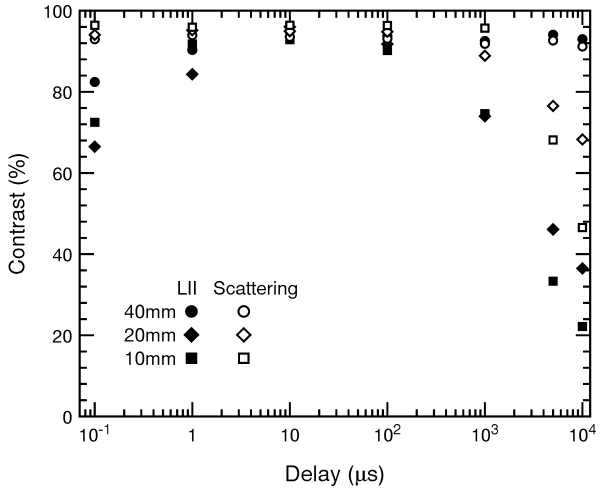

Figure 9. Lifetime of the vaporized soot "hole" in the laminar diffusion flame based on the change in contrast with delay time between the marking and readout lasers, for a marking laser fluence of 7.8 J/cm^2. Results are shown for three flame heights and for both LII and scattering detection.

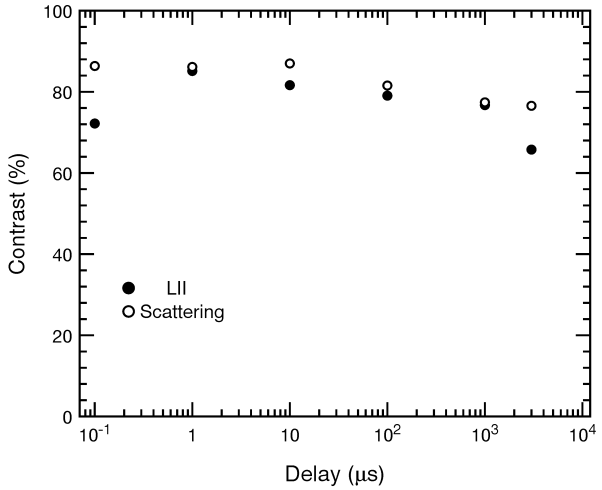

Figure 10. Lifetime of the vaporized soot "hole" in the soot generator (0.7 ppb soot loading) for a marking laser fluence of 7.8 J/cm^2.

The behavior in the lower regions of the flame (10 and 20 mm) is quite different. There the contrast begins to degrade after ~100 μs, although it remains above 20% even at 10 ms. These lower locations in the flame are within the region where new soot particles are formed from large hydrocarbon molecules.[27] Thus the vaporized soot particles can be (slowly) replaced with new particles. In these regions, the scattering contrast falls less rapidly than the LII contrast. In other words, the LII signal returns faster than the scattering signal. This is consistent with the formation of new, small soot particles or growth of the very small particles that likely remain after the marking laser pulse. LII is a more sensitive method for detecting these small particles, and should therefore be influenced first.

For short time delays (≤ 1 μs), the scattering results produce high contrast levels, while the LII detection shows a reduction in contrast (compared to the intermediate time delays). This is seen in both the flame and soot generator results. The LII contrast loss is associated with interference from the marking laser pulse. While the central part of the marking laser vaporizes the soot particles in its path, the lower energy wings are not sufficient to remove the soot. They can, however, heat the soot particles sufficiently to induce a strong LII signal, which has a lifetime between 100 ns and 1 μs (limited by the cooling rate of the heated particles). The LII produced by the marking laser from these particles in the side edges and vertical wings of the horizontal sheet can therefore be detected in LII images acquired with delays of ~1 μs or less. The LII interference is negligible compared to the much strong scattering signal.

Summary

We have described an approach for particle velocity measurements that can be applied to absorbing particles, even at high particle loading. The technique requirements are relatively simple, requiring at least one pulsed (but not tunable) laser for marking. *Scattering interrogation* could be carried out with a bright pulsed light source, or even a continuous wave laser and a fast, gated detector. Scattering detection provides a higher signal, though it may be susceptible to interferences from scattering, nonabsorbing particles (or other scattering surfaces). In addition, the technique can easily be adapted for appropriate particles, to achieve local particle mass flux measurements by monitoring LII from the marking pulse.

The laser fluence required to produce the tagged region for soot is on the order of the LII threshold fluence. For both scattering and LII detection, maximum tag contrast is attained for a fluence 3-4 times the LII threshold level (~1.5-2 J/cm^2 compared to a threshold of 0.6 J/cm^2 for a 1064 nm Nd:YAG laser). While LII detection requires a fluence above the threshold value to produce a measurable contrast, scattering detection gives easily detectable contrasts at fluences below the threshold. Scattering from the soot is more sensitive to

particle size reductions (or other changes in the soot structure) compared to LII.

The lifetime of the marked region for soot particles is generally quite long. In the slightly unsteady, nonreacting jet, the lifetime is well in excess of 3 ms. As expected, particle diffusivity is quite slow and does not limit the tag lifetime. In the lower regions of the flame, where soot inception is rapid, the lifetime also exceeds 3 ms. This suggests that in most practical, soot-containing flows (reacting and nonreacting), the tag lifetime will be limited by turbulent mixing. Since turbulence levels typically scale with the mean velocity, i.e., lower mean velocities correspond to smaller velocity fluctuations, the tag lifetime will scale with the velocity of the flow (faster flows=shorter lifetimes). However, the required tag lifetime (which is determined by the time needed for the tag to move some number of pixels) is inversely proportional to the flow velocity. Therefore PVV should be applicable over a wide range of flow velocities.

Acknowledgments

Portions of this work were supported by the National Science Foundation under a CAREER award (CTS-9502371) and by MetroLaser, Inc. under a Department of Defense (Arnold Air Force Base) Phase II Small Business Innovative Research Program.

References

[1]I. K. Puri, *Environmental Implications of Combustion Processes*, CRC Press, Boca Raton, FL, 1993.

[2]R. Wilson and J. D. Spengler, ed., Particles in Our Air: Concentrations and Health Effects, Harvard University Press, 1996.

[3]M. Kleeman and G. Cass, "Source Contributions to the Size and Composition Distribution of Urban Particulate Air Pollution," Atmospheric Environment **32**, No. 16, 2803-2816 (1998).

[4]C. Arcoumanis, P. Cutter, D. S. Whitelaw, "Heat Transfer Processes in Diesel Engines," Chem. Eng. Res. Des. **76,** 124-132 (1998).

[5]Dobbins, R. A., Fletcher, R. A., and Lu, W., "Laser Microprobe Analysis of Soot Precursor Particles and Carbonaceous Soot", Combustion and Flame **100**, 301-309 (1995).

[6]Köylü, Ü. Ö., McEnally, C. S., Rosner, D.E., and Pfefferle, L. D., "Simultaneous Measurements of Soot Volume Fraction and Particle Size/Microstructure in Flames Using a Thermophoretic Sampling Technique," Combustion and Flame **110**, 494-507 (1997).

[7]Puri, R., Richardson, T. F., Santoro, R. J., and Dobbins, R. A., "Aerosol Dynamic Processes of Soot Aggregates in a Laminar Ethene Diffusion Flame," Combustion and Flame **92**, 320-333 (1993).

[8]Santoro, R. J., Yeh, T. T., Horvath, J. J., and Semerjian, H. G., "The Transport and Growth of Soot Particles in Laminar Diffusion Flames," Combustion Science and Technology **53**, 89-115 (1987).

[9]Vander Wal, R. L., and Weiland, K. J., "Laser-Induced Incandescence: Development and Characterization Towards a Measurement of Soot-Volume Fraction," Applied Physics B **59**, 445-452 (1994).

[10]Quay, B., Lee, T. W., Ni, T., and Santoro, R. J., "Spatially Resolved Measurements of Soot Volume Fraction Using Laser-Induced Incandescence," Combustion and Flame **97**, 384-392 (1994).

[11]Shaddix, C. and Smyth, K., "Laser-Induced Incandescence Measurements of Soot Production in Steady and Flickering Methane, Propane, and Ethylene Diffusion Flames," Combustion and Flame **107**, 418-452 (1996).

[12]Vander Wal, R. L. and Dietrich, D. L., "Laser-Induced Incandescence Applied to Droplet Combustion," Applied Optics **34**, 1103-1107 (1995).

[13]Dec, J. E., zur Loye, A. O., and Siebers, D. L., "Soot Distribution in a D.I. Diesel Engine Using 2-D Laser-Induced Incandescence," SAE Paper 910224 (1991).

[14]Pinson, J. A., Mitchell, D. L., Santoro, R. J., Litzinger, T. A., "Quantitative, Planar Soot Measurements in a D.I. Diesel Engine Using Laser-Induced Incandescence and Light Scattering," SAE Paper 932650, (1993).

[15]Case, M. E., and Hofeldt, D. L., "Soot Mass Concentration Measurements in Diesel Engine Exhaust Using Laser-Induced Incandescence," Aerosol Science and Technology **25**, 46-60 (1996).

[16]Wainner, R. T., Seitzman, J. M., and Martin, S. R. "Soot Measurements in a Simulated Engine Exhaust using Laser-Induced Incandescence," AIAA Journal **37**, 738-743 (1999).

[17]Snelling, D. R., Smallwood, G. J. Sawchuk, R. A., Neill, W. S., Gareau, D. Chippior, W. L., Liu, F., Gülder, Ö. L. and Bachalo, W. D., "Particulate Matter Measurements in a Diesel Engine Exhaust by Laser-Induced Incandescence and the Standard Gravimetric Procedure," SAE Paper 1999-01-3653 (1999).

[18]Will, S., Schraml, S., and Leipertz, A., "Two-dimensional Soot Particle Sizing by Time-resolved

Laser-induced Incandescence," Optics Letters **20**, 2342-2344 (1995).

[19]Mewes, B., and Seitzman, J. M., "Soot Volume Fraction and Particle Size Measurements with Laser-Induced Incandescence," Applied Optics **36**, 709-717 (1997).

[20]Taylor, A. M. K. P. ed., *Instrumentation for Flows with Combustion*, Academic Press, London, 1993.

[21]Willert, C. E. and Gharib, M., "Digital Particle Image Velocimetry," Experiments in Fluids **10**, 181-193 (1991).

[22]Buchhave, P., "Particle Image Velocimetry - Status and Trends," Experimental Thermal and Fluid Science **5**, 586-604 (1992).

[23]Miles, R. B., Zhou, D., Zhang, B., Lempert, W. R. and She, Z., "Fundamental Turbulence Measurements by Relief Flow Tagging," AIAA Journal **31**, 447-452 (1993).

[24]Pitz, R. W., Brown, T. M., Nandula, S. P., Skaggs, P. A., DeBarber, P. A. and Brown, M. S., "Unseeded Velocity Measurement by Ozone Tagging Velocimetry," Optics Letters **21**, 755-757 (1996).

[25]Stier, B. and Koochesfahani, M. M., "Molecular Tagging Velocimetry (MTV) Measurements in Gas Phase Flows," Experiments in Fluids **26**, 297-304 (1999).

[26]Dasch, C. J., "Continuous-Wave Probe Laser Investigation of Laser Vaporization of Small Soot Particles in a Flame," Applied Optics **23**, 2209-2215 (1984).

[27]Santoro, R. J., Yeh, T. T., Horvath, J. J. and Semerjian, H. G., "The Transport and Growth of Soot Particles in Laminar Diffusion Flames," Combustion Science and Technology **53**, 89-115 (1987).